Cellular Physiology and Biochemistry

Cell Physiol Biochem 2018;48:348-360
DOI: 10.1159/000491741
Published online: July 16, 2018
Accepted: May 04, 2018

Original Paper

MicroRNA-141 Inhibits the Proliferation of Penile Cavernous Smooth Muscle Cells Associated with Down-Regulation of the Rhoa/Rho Kinase Signaling Pathway

Ying Zhang[a] Linpei Jia[b] Wei Ji[c] Hai Li[d]

[a]Department of Pathology, China-Japan Union Hospital of Jilin University, Changchun, [b]Department of Nephrology, Xuanwu Hospital, Capital Medical University, Beijing, [c]Department of Vascular Surgery, Jilin Provincial People's Hospital, Changchun, [d]Department of Urology, China-Japan Union Hospital of Jilin University, Changchun, P.R. China

Key Words
Microrna-141 • Diabetes mellitus erectile dysfunction • RhoA/Rho kinase signaling pathway • Rho • Rho kinase II

Abstract
Background/Aims: The role of the RhoA/Rho kinase signaling pathway in diabetes mellitus-induced erectile dysfunction has been partially understood. ***Methods:*** In the present study, we explored the changes of the RhoA/Rho associated kinase (ROCK) signaling pathway in diabetic erectile dysfunction *in vivo* and the effects of microRNA-141 on the RhoA/ROCK signaling pathway *in vitro*. ***Results:*** The mRNA and protein expressions of RhoA and ROCK2 were significantly increased while the expression of microRNA-141 was decreased in the penile cavernous smooth muscle cells of rats with diabetic erectile dysfunction. Moreover, increased expression of microRNA-141, decreased expressions of RhoA and ROCK2 (mRNA and protein), accelerated cell proliferation rate and reduced cell apoptosis were found in the microRNA-141 mimics group and the siRNA-Rho group. The microRNA-141 expression in the microRNA-141 inhibitors + siRNA-Rho group was significantly decreased. microRNA-141 specifically bound to Rho-3'-UTR and down-regulated the expression of Rho gene at the post transcriptional level. ***Conclusion:*** Decreased expression of miR-141 is associated with up-regulation of RhoA and ROCK2 in the RhoA/ROCK signaling pathway in rats with diabetic erectile dysfunction. miR-141 inhibits the growth of penile cavernous smooth muscle cells associated with down-regulation of the RhoA/ROCK signaling pathway *in vitro*.

Introduction

Patients with diabetes mellitus (DM) are subject to chronic complications with increasing morbidity and mortality [1, 2]. Erectile dysfunction (ED) refers to the inability to keep the penile erection for a kind of sexual behavior [3]. As one of the complications

Dr. Hai Li
Department of Urology, China-Japan Union Hospital of Jilin University
No. 126, Xiantai Street, 130033 Changchun, Jilin Province, (P.R. China)
Tel. +86-431-84995138, E-Mail muandkamu_2012@aliyun.com

of DM, ED generally occurs in elderly patients [4]. Additionally, orgasmic dysfunction is often associated with ED patients combined with type 2 diabetes mellitus (T2DM) [5]. Low testosterone levels may partially account for the pathogenesis of DMED; a recent study showed that men with T2DM had a low testosterone level that may lead to low sex drive and ED [6]. Furthermore, other factors including old age and low penile blood flow may also contribute to the occurrence of DM-induced ED (DMED) [7].

Rho associated kinase (ROCK) is a serine/threonine kinase that interacts with activated Rho GTPases and the RhoA/ROCK signaling pathways control an extensive essential cell functions, including cell adhesion, motility, proliferation, differentiation, and apoptosis [8]. ROCK2 was significantly up-regulated in the cavernous smooth muscle cells and/or myofibroblasts of patients with ED, and ROCK1 inhibitor Y-27632 caused a significant relaxation of corpus cavernosum in tissue strips of patients with severe ED [9].

microRNA (miR) is a kind of short non-coding RNA, which acts as an evolutionarily conserved regulator of gene expression [10]. miR is a single stranded RNA molecule with a length of about 18-23 nucleotides and exerts its functions in regulating gene expression by pairing base-pairing with the 3' untranslated region of the target mRNA [11]. The role of miR in DMED has been scarcely studied. Li et al. showed that miR-328 antagomir could improve ED in streptozotocin (STZ)-induced diabetic rats [12]. A previous study indicated that the inhibition of miR-141 was associated with cell cycle, apoptosis, growth, migration and invasion in cancer cells; bromodomain-containing protein (BRD)3, ubiquitin-associated protein (UBAP)1 and phosphatase and tensin homolog (PTEN) were potential targets of miR-141 [13]. Over-expression of miR-141 decreased mitochondrial superoxide dismutase and catalase activities, and increased reactive oxygen species (ROS) levels in cardiomyocytes exposed to glucose fluctuations [14].

Over-expression of miR-200a was recognized in the corpus cavernosum tissues of rats with aging-related ED and the chief target pathway was endothelial nitric oxide synthase (eNOS)/nitric oxide (NO)/protein kinase G (PKG), which is an important pathway involved in the physiology of normal erection [15]. Thus far, the role of the RhoA/ROCK signaling pathway in DMED has been partially understood and the mechanism of miR in DMED is unclear. Thus, we aim to probe into the effect of miR-141 on DMED by targeting the RhoA/ROCK pathway in rats with DM.

Materials and Methods

Ethics statement

The study protocol was approved by the Committee on the Ethics of China-Japan Union Hospital of Jilin University. This study was conducted in strict accordance with the guidelines for both the care and use of laboratory animals. All efforts were made to minimize the number of animals used and their sufferings.

Animals and grouping

Specific pathogen free (SPF) male Sprague-Dawlay (SD) rats were purchased from the Slac Laboratory Animal Company (Shanghai, China) and were housed on a 12/12 light-dark schedule with water and food available *ad libitum*. Detailed accommodation and care complied with Chinese recommendations and legislations. Ninety-five rats at 10-week old with mean body weight 287.8g were selected for our experiments. The mating test showed that the sexual function of all rats was normal. Twenty rats were randomly selected as the normal group and another 75 into the observation group.

Construction of the DMED model

After fasted for 8-12 h, rats were intraperitoneally injected with STZ (40 mg/kg) (Sigma, USA) to induce the DM model. Symptoms were recorded of after STZ injection, and tail-cutting method and Roche blood glucose meter (Roche Company, Germany) were daily performed to detect the blood glucose level from the fourth day. The model was successfully established when the random serum glucose level reached

more than 16.67 mmol/L. The blood glucose level was measured once a week and when the value reached over 25 mmol/L, 2IU protamine zinc insulin was injected subcutaneously to rats. DM rats were placed into the metal cages and fed for 10 weeks. A total of 100 g/kg apomorphine hydrochloride (APO) (Shenyang First Pharmaceutical Factory, Shenyang, China) was injected into the soft skin of neck by subcutaneous injection. Rats were observed by a video recorder from the bottom of the cage for 30 min and the erection times were recorded. The standards of penile erection in rats: the prepuce was receded, and the penis was enlarged and the glans was exposed. Rats without penile erection were used as DMED rats. The penile cavernous bodies were removed when all animals were sacrificed at the end of 12 weeks after modeling. A total of 10 penile cavernous bodies were fixed with 4% paraformaldehyde, and embedded with paraffin, and cut into serial sections. The remaining samples were snap-frozen with liquid nitrogen and then stored at -80°C.

Hematoxylin-eosin (HE) staining and Masson staining

Neurovascular tissues in suspensory ligament of phalange and proximal and distal tissues in nervus dorsalis of penis were extracted. Samples were fixed with 4% paraformaldehyde for 24 h; the corpus cavernosum tissues were removed from the fixative solution. Routine dehydration (once for 1 min) with gradient alcohol of 70%, 80%, 90%, 95%, and 100%, xylene transparenting (twice for 5 min), wax dipping and paraffin embedding were done and 5 μm paraffin sections were taken. The dimethylbenzene dewaxing of slices were performed, after which were spread and fished at 45°C and baked at 60°C. The HE staining was performed, followed by gradient alcohol dehydration and xylene transparenting, and then all slides were mounted with neutral balata. The Masson staining was used to distinguish cells from surrounding connective tissue. Pathological changes of spongy tissues of corpus cavernosum were observed using a light microscope (Olympus, Japan).

Immunohistochemistry

The samples were firstly fixed with paraformaldehyde and embedded with paraffin with a thickness of 4 μm. Tissues were incubated at 60°C for 1 h, after the procedures of the conventional xylene dewaxing together with the gradient alcohol dehydration, samples were placed into the 3% H_2O_2 for 10 min, washed with distilled water for 3 times and each time for 3 min. Samples were repaired for 90 s with high pressure antigen, bathed with cold water and cooled into room temperature, and phosphate buffer saline (PBS) washing was done for 3 times (3 min each time). Bovine serum albumin (BSA) blocking solution was added into samples and the samples were incubated at 37°C for 30 min. Slices were removed and dried, and added into rabbit monoclonal antibodies RhoA (1:1000, Abcam, Cambridge, UK) at 4°C overnight. Slices were rinsed with PBS for 3 times (3 min each time). The secondary antibody of sheep anti-rabbit RhoA (1:2000, Abcam, Cambridge, UK) was added into samples and incubated at 37°C for 30 min. Samples were washed with PBS for 3 times (3 min each time). Streptomycin avidin-peroxidase solution (ZSGB Biotechnology Co., Ltd., Beijing, China) was added into samples and were incubated at 37°C for 30 min. Diaminobenzidine (DAB) staining solution (Bioss Biotechnology Co., Ltd., Beijing, China) was added. The reaction was terminated by using water. All slices were displayed on shelf after their color displayed, and socked into purified water for 5 min. Samples were washed with hematoxylin for 5 min and then washed with tap water. Slices were removed and rinsed with 1% hydrochloric alcohol and stained in blue with tap water for 20 min. Staining results were divided into two kinds: positive and negative. Positive staining was found in the cytoplasm and nucleus of cells showing brown yellow granular, and negative staining was found in the cytoplasm and nucleus of cells without showing brown yellow granular. Positive expression rate = positive cells number/ total cells number X 100%.

Quantitative real-time polymerase chain reaction (qRT-PCR)

Total RNAs from corpus cavernosum tissues of rats in each group were extracted by Kit (Invitrogen Company, Shanghai, China). After identifying the purity and integrity of RNA, miR-141, RhoA, ROCK1, ROCK2 primers were designed and synthesized by TaKaRa company (Dalian, China). The RNA template, Primer Mix, dNTP Mix, DTT, RT Buffer, HiFi-MMLV, and enzyme without RNA were placed on the ice and dissolved for further use. The system of 20 μL was reversely transcripted according to TaqMan MicroRNA Assays Reverse TranscriptioN Primer (Thermo Fisher Scientific), the reaction conditions were as follows: 42°C for 30-50 min (reverse transcription reaction) and 85°C for 5 s (enzyme inactivation reaction of reverse transcriptase). The reaction solution was taken for qRT-PCR by referring to KIT SYBR Premix Ex TaqTM

II kit (RR820A, Action-Award Biological Technology Co. Ltd.) instructions for quantitative PCR operation. The reaction condition was: 40 cycles of predenaturation at 95°C for 10 min, denaturation at 95°C for 10 s, annealing at 60°C for 20 s, and extending at 72°C for 34 s. The reaction system was: 10 μL SYBR Premix Ex TaqTM II, 0.8 μL PCR Forward Primer (10 μM), 0.8 μL PCR Reverse Primer (10 μM), 0.4 μL ROX Reference Dye and 2.0 μL cDNA template, and 6.0 μL sterile purified water. The U6 was used as internal reference of miR-141, and β-actin (Absin Bioscience Inc., Shanghai, China) acted as internal reference of RhoA, ROCK 1 and ROCK 2. $2^{-\Delta\Delta Ct}$ was the ratio of gene expression of experimental group and the control group, the formula was as follows:$\Delta\Delta CT = \Delta Ct_{(experimental\ group)} - \Delta Ct_{(control\ group)}$, of which $\Delta Ct = Ct_{miRNA} - Ct_{RhoA}$. Ct was the number of amplification cycles when the real time fluorescence intensity of the reaction reached a threshold value, and the amplification corresponded to logarithmic growth (Table 1).

Western blotting

Liquid nitrogen was added into the penile cavernous smooth muscle cells, and it was grinded until the tissues showed fine powder uniformly. Then the protein lysate was placed on ice, grinded into homogenates and vortexed once every 10 min. Supernatants were obtained to determine the protein concentration by the bicinchoninic acid (BCA) method (20201ES76, Yi Sheng Biotechnology Co. Ltd, Shanghai, China). The grease layer was abandoned and centrifuged at 2000 X g and 4°C for 20 min. Proteins were measured and the deionized water was adjusted to ensure that the sample loading was consistent. About 10% sodium dodecyl sulfate (SDS) separation gel and concentration gel were allocated. Samples were mixed with the loading buffer, boiled at 100°C for 5 min, and added into each lane for ionophortic separation with a micropipette after ice bath and centrifugation. Then the protein was transferred protein in gel to nitrocellulose filter (NC filter). 5% skimmed milk powder was sealed off with NC filter at 4°C overnight. The primary antibody (rabbit monoclonal antibodies, namely anti-RhoA (1:1000), anti-ROCK (1:500), anti-ROCK 2 (1:250) and anti-β-actin (1:1000), all from Abcam, Cambridge, UK) were incubated overnight at room temperature, washed with PBS for 3 times (5 min each time). Goat anti-rabbit IgG (1:1000, Boster Company, Wuhan, China) labeled with horseradish peroxidase was supplemented, and then the secondary antibody was incubated at 37°C for 1 h. Samples were rinsed with PBS at room temperature for 3 times (5 min each time). The NC filter was immersed in electrochemiluminescence (ECL) solution (Pierce company, USA) at room temperature for 1 min. The results were observed after development and fixation. β-actin served as the internal reference, and the relative expressions of protein were expressed as the ratio of gray value of target band and internal reference band.

Cell culture

The penis of DMED rats were taken from the lower edge of phalanx under aseptic condition, and the tunica albuginea and urethra of penis were removed as much as possible. Corpora cavernosum penis were transferred into a Petri-dish containing a small amount of Dulbecco's modification of essential medium (DMEM) and washed with PBS for 3 times, tissue blocks were sheared to 1 mm^3 and washed with PBS again. Cells were cultured in RPMI 1640 medium (Gibco, Gaitherburg, MD, USA) containing 10% fetal bovine serum (FBS) (Gibco, Gaitherburg, MD, USA) at 37°C with 5% CO_2. Single cell suspension was obtained by digesting tissues with 0.25% trypsin (Gibco, Gaitherburg, MD, USA). Then cells were cultured and passaged conventionally. Finally, cells in the logarithmic growth phase were used for further experiments.

Cell transfection

Cells in the logarithmic growth phase of the cavernous tissues of rats were inoculated in a 6-well plate, and the cell density was increased to 30%-50%. The cells were transfected according to instructions of lipofectamin 2000 (Invitrogen Corp., USA). Opti-MEM serum-free medium (250

Table 1. Primers sequences of quantitative real-time polymerase chain reaction (qRT-PCR). Notes: ROCK: Rho-associated protein kinase; F, forward; R, reverse

Gene	Gene sequences
miR-141	R: 5'-CAUCUUCCAGUACAGUGUUGGA -3'
	F: 5'-UAACACUGUCUGGUAAAGAUGG -3'
U6	R: 5'-CTCGCTTCGGCAGCACA-3'
	F: 5'-AACGTTCACGAATTTGCGT-3'
RhoA	R: 5'-TGACCGCCTGTAGCCTTGAC -3'
	F: 5'-CCCACTCGCCCTGATTTATG -3'
ROCK 1	R: 5'-TGATGGCTATTATGGACGAG -3'
	F: 5'-GGAGCGTTTCCCAAGC -3'
ROCK 2	R: 5'-CCTGTCAAGCGTGGTAGTGA -3'
	F: 5'-TTAGTGTTGTTCCGCACAGG -3'
β-actin	R: 5'-AGGGAAATCGTGCGTGAC-3'
	F: 5'-ACCCAGGAAGGAAGGCT-3'

μL) (Gibco, NY, USA) was used to dilute 100 pmol plasmids in the NC group, miR-141 diluted inhibitors, miR-141 mimics, miR-141 inhibitors + siRNA-Rho groups (diluted the final concentration of each cell is 50 nM), vortexed gently and incubated at room temperature for 5 min; 250 μL serum-free Opti-MEM medium was used to dilute 5 μL lipofectamin 2000, vortexed gently and incubated at room temperature for 5 min. The two samples were mixed, incubated at room temperature for 20 min and added into the cell culture wells. Mixed cells were cultured at 37°C with 5% CO_2 for 6-8 h. After another 24-48 h, cultured cells were used for subsequent experiments.

Luciferase reporter gene assay

Biological prediction website microRNA.org showed that miR-141 can target Rho. Luciferase reporter gene assay was performed to verify whether Rho was a direct target of miR-141. The artificially synthesized Rho 3'UTR were introduced into the pMIR-reporter by restriction site of Spel and Hind III, and the mutant (MUT) site of complementary sequence of seed sequence was designed on the basis of the Rho wild type (WT). After digestion with restriction endonuclease, the target segments were inserted into the pMIR-reporter plasmid byT4 DNA ligase. The plasmids (WT and MUT), which were sequenced correctly, were transfected into HEK-293T cells by co-transfection with miR-141. After 48 h transfection, the cells were collected and lysed, and the luciferase activity was detected by the luciferase assay kit (Genomeditech, China).

3-(4, 5-dimethylthiazol-2-yl)2, 5-diphenyl tetrazolium bromide (MTT) assay

The corpus cavernosum tissues at the logarithmic growth phase were collected, washed with PBS for twice and digested with 0.25% trypsin when the cell density reached about 80% after transfection. Cell suspension at 2.5 X 10^5/mL was prepared with RPMI1640 containing 10%FBS. Cells were inoculated into 96-well culture plates and cultured. The culture plates were removed at 24 h, 48 h and 72 h, respectively, and 5 mg/mL MTT (Sigma-Aldrich, St. Louis, MO, USA) solution were added into each well for 4 h, and then the optical density (OD) value at 490 mm was measured by an automatic microplate reader.

Flow cytometry

Cells were collected after 48 h transfection and digested with 0.25% trypsin solution. The concentration of sample cells was adjusted to 1 X 10^6/mL cells (1 mL). The pre-cooling alcohol solution (volume fraction was 70%) was used to fix cells at 4°C overnight. Cells were washed with PBS for twice the next day, and 1 ml 50 mg/L propidium iodide (PI) dye liquor (containing RNAase) was added. Cells were placed in the dark for 30 min, and then filtered with nylon mesh filters. Flow cytometry (FACS Calibur, Becton and Dickinson Company, New Jersey, USA) was performed to record the cell cycles. Apoptosis was detected by Annexin V-FITC/PI double staining. Cells were cultured in an incubator at 37°C with 5% CO_2 for 48 h. Cells were collected and then rinsed with PBS for twice. The cells were resuspended into 200 μL binding buffer after centrifugation. 10 μL Annexin V-FITC and 5 μL PI solution were added for detecting the cell apoptosis at the excitation wave-length of 488 nm with flow cytometry.

Statistics

Data were presented as mean values ± standard deviations (SD). The Statistical Program for Social Sciences (SPSS) 21.0 software (SPSS, IBM, West Grove, PA, USA) was used for data analysis. The one-way analysis of variance (ANOVA) and the Kruskal-Wallis test were used to compare values among groups followed by the Student's t-test or the Mann-Whitney U-test to compare values between groups. The Pearson correlation analysis was carried out for the analysis of the correlation of two variable quantities. All tests were two-tailed, with the level of significance set to $P < 0.05$.

Results

Successful establishment of the DMED model

We found that modeling rate of DM was low when rats were injected with STZ at the dosage of 35 mg/kg per time, and the mortality rate would increase when rats were injected with STZ at the dosage of 60 mg/kg per time. No rats died when they were injected with STZ

at the dosage of 40 mg/kg, and all developed DM. Thus, the optimal dosage was set to 40 mg/kg. The weight and blood glucose level of rats were shown in Table 2. The body weight in the DMED group was obviously lower in comparison with the normal group (all $P < 0.05$). After the normal and the DM rats were injected with apomorphine hydrochloride, the penile erection rates of diabetic rats were obviously reduced at the 10th week as compared with the normal controls (all $P < 0.05$).

Pathological changes of the corpus cavernosum tissues in DMED

HE staining showed that in the normal group, penile corpora cavernosum contained a large number of sinusoids; the trabecula of sinusoid contained a large number of collagen fibers and smooth muscles (Fig. 1A). The DMED group presented increased collagen fiber density in the penile corpora cavernosum, thickened penile vascular wall, and decreased number of smooth muscles and irregular lumen. In the normal group, cavernous sinusoids were distributed regularly, cavernous smooth muscle (Masson staining was red) were arranged according rules. The penis of rats in the DMED group became smaller, the number of sinusoids were reduced, and stromal component (Masson staining was green) were increased (Fig. 1B).

Expression of RhoA was up-regulated in the corpus cavernosum tissues of rats with DMED

Immunohistochemistry was used to detect the expression of RhoA in the corpus cavernosum tissues of rats with DMED. The expression of RhoA protein was strongly positive in the penile corpus cavernosum tissues of rats in the DMED group, and was weakly positive or negative in rats of the normal group (Fig. 1C). Compared with the normal group, the expression of RhoA protein in the penile corpus cavernosum tissues of rats in the DMED group was significantly up-regulated (Fig. 1D).

miR-141 was down-regulated and mRNA of RhoA and ROCK2 was up-regulated in DMEM

qRT-PCR was used to detect the expressions of miR-141 and mRNA expressions of related proteins in the RhoA/ROCK signaling pathway in the penile corpus cavernosum tissues of rats. The expression of miR-141 in the DMED group was remarkably lower than that in the normal group ($P < 0.05$). Compared with the normal group, the mRNA expressions of RhoA and ROCK2 were significantly higher in the DMED group (both $P < 0.05$), while there was no statistical significance in the mRNA expression of ROCK1 between the two groups ($P > 0.05$) (Fig. 2A).

Expressions of RhoA and ROCK2 protein were increased in DMED

The protein expressions of RhoA, ROCK1 and ROCK2 in the penile corpus cavernosum tissues of rats were detected by Western blotting. Compared with the normal group, the expressions of RhoA and ROCK 2 protein were significantly increased in the penile corpus cavernosum tissues of rats in the DMED group (both $P < 0.05$), the expression of ROCK1

Table 2. Changes of blood glucose level and body weight of rats before and after DM modeling. DM, diabetes mellitus. *, P < 0.05 compared with the normal group; #, P < 0.05 compared with 4 d after modeling. The body weight and blood glucose levels in the table refer to diabetic rats only

			Day 4 after modeling		Day 10 after modeling	
Group	Incidence of DM	Weight (g)	Weight (g)	Blood glucose (mmol/L)	Weight (g)	Blood glucose (mmol/L)
Normal	0/20	286.4 ± 19.2	301.2 ± 19.1	3.85 ± 0.78	389.1 ± 20.1#	6.68 ± 0.88#
35 mg/kg DM	5/20	289.7 ± 18.8	289.1 ± 18.9	20.65 ± 3.01*	224.7 ± 16.6*#	23.81 ± 3.65*#
40 mg/kg DM	25/25	287.8 ± 18.5	287.2 ± 20.3	21.65 ± 3.99*	230.6 ± 17.7*#	25.22 ± 3.11*#
60 mg/kg DM	19(6 dead)	291.1 ± 19.6	288.6 ± 19.3	23.21 ± 3.88*	226.1 ± 18.8*#	25.84 ± 3.77*#

protein showed insignificant difference between two groups ($P > 0.05$) (Fig. 2B and 2C).

miR-141 specifically binds to Rho-3'-UTR and down-regulates the expression of Rho gene at the post transcriptional level

Online analysis software showed that there was a specific binding region between Rho3'UTR and miR-141 sequences, and Rho was the target gene of miR-141 (Fig. 3A). The luciferase reporter gene assay was performed to verify whether Rho was the target of miR-141 (Fig. 3B). The luciferase activity of Rho WT 3'UTR was significantly suppressed in the miR-141mimics group ($P < 0.05$), while the MUT 3'UTR luciferase activity was not inhibited. These results suggest that miR-141 may specifically bind to Rho-3'-UTR and down-regulate the expression of Rho gene at the post transcriptional level.

miR-141 levels were down-regulated and mRNA expressions of RhoA and ROCK2 were up-regulated in culture cells

The expression of miR-141 in other groups was significantly decreased as compared with the normal group, and the mRNA expressions of RhoA and ROCK2 were significantly increased (all $P < 0.05$). The mRNA expression of related proteins in the RhoA/ROCK signaling pathway and miR-141 expression showed in significant difference in comparison with the blank group and NC group (all $P > 0.05$). Compared with the blank group and the NC group, the expression of miR-141 in the miR-141 mimics group was significantly increased, the expression of miR-141 had no difference in the siRNA-Rho group ($P > 0.05$), and the expression of RhoA and ROCK2 mRNA were significantly reduced

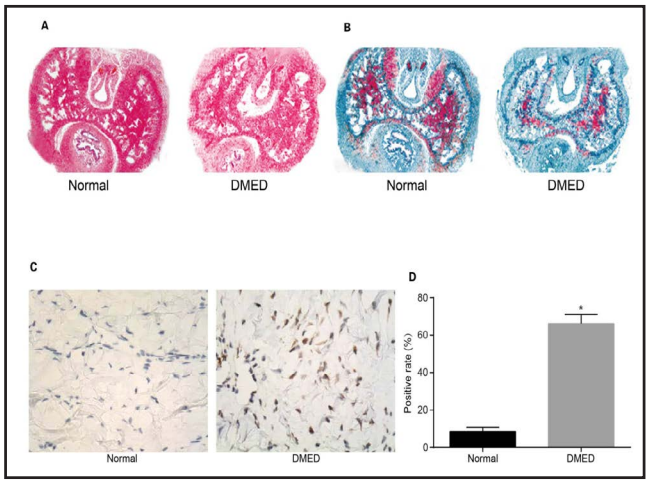

Fig. 1. The penile cavernous smooth muscle cells of rats between normal and DMED groups by HE/Masson staining (X 200). A: HE staining for normal rats and DMED rats;B: Masson staining for normal rats and DMED rats; C: The positive rate of the RhoA protein in the penile corpus cavernosum tissues in the normal and DMED groups, immunohistochemical staining of Rho protein; D: statistical analysis of the positive rate of RhoA protein expression. * P<0.05 compared with the rats in the normal group.

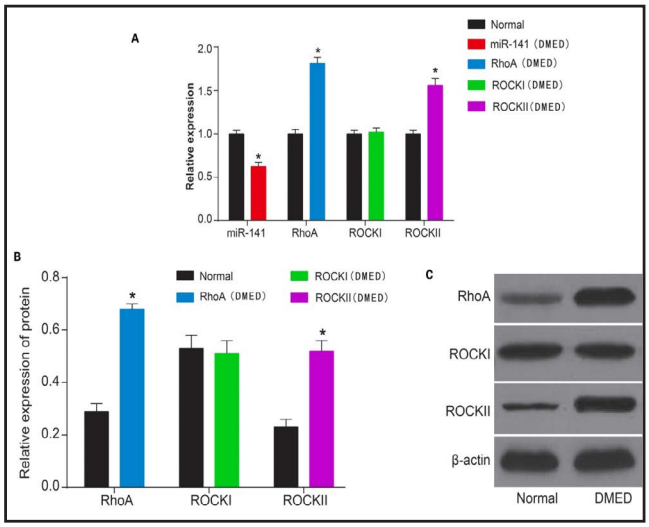

Fig. 2. Expressions of miR-141 and mRNA expressions of related proteins in the RhoA/ROCK signaling pathway in the penile corpus cavernosum tissues of rats. A: protein expressions of RhoA, ROCK1 and ROCK2 in the penile corpus cavernosum tissues of rats; B: statistical analysis chart for protein expressions of RhoA, ROCK1 and ROCK2 in the penile corpus cavernosum tissues of rats; C: western blotting for protein expressions of RhoA, ROCK1 and ROCK2 in the penile corpus cavernosum tissues of rats. * P<0.05 compared with the normal group.

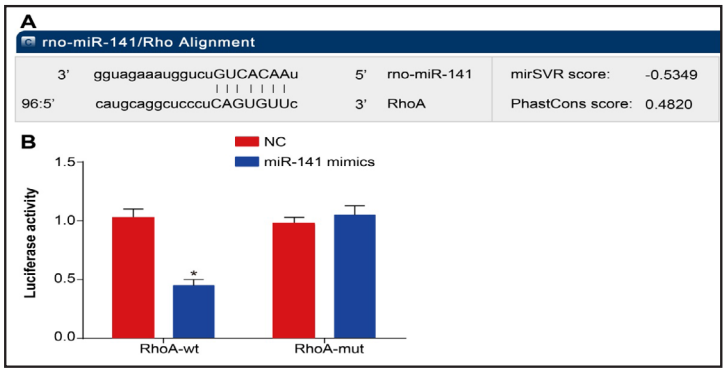

Fig. 3. Relationship between Rho gene and miR-141. Online analysis software showed that there was a specific binding region between Rho3'UTR and miR-141 sequences, and Rho was the target gene of miR-141 (A). The luciferase reporter gene assay was performed to verify whether Rho was the target of miR-141. The luciferase activity of Rho WT 3'UTR was significantly suppressed in the miR-141mimics group as compared to the NC group, (P<0.05), while the MUT 3'UTR luciferase activity was not inhibited (B). These results suggest that miR-141 may specifically bind to Rho-3'-UTR and down-regulate the expression of Rho gene at the post transcriptional level. * P<0.05 compared with the NC group.

in the miR-141 mimics group and the siRNA-Rho group (all $P < 0.05$); miR-141 expression in the miR-141 inhibitors group was decreased, and the mRNA expressions of RhoA and ROCK2 were significantly increased (all $P < 0.05$), the expression of miR-141 in the inhibitor + siRNA-Rho group was significantly lowered ($P < 0.05$), while the mRNA expressions of RhoA and ROCK2 were unaltered (both $P > 0.05$). No significant difference was detected in mRNA expression of ROCK1 in cells of each group (all $P > 0.05$) (Fig. 4A).

Expressions of RhoA and ROCK 2 protein were increased in cultured cells

Compared with the normal group, the expressions of RhoA and ROCK2 protein as detected by Western blotting were markedly increased in other groups (all $P < 0.05$). The expressions of the RhoA/ROCK signal pathway related proteins were insignificantly different between the blank group and the NC group (all $P > 0.05$). Compared with the blank and the NC groups, the expressions of RhoA and ROCK2 protein in the miR-141 mimics group and the siRNA-Rho group were significantly decreased, while in the miR-141 inhibitors group was significantly increased ($P < 0.05$). The expressions of RhoA and ROCK2 protein in the miR-141 inhibitors + siRNA-Rho group showed insignificant changes (both $P > 0.05$). No significant difference was found in the expression of ROCK1 protein among groups (all $P > 0.05$) (Fig. 4B and 4C).

Proliferation ability after cell transfection

Compared with the normal group, cell proliferation was significantly decreased in other groups. No significant difference was detected in the blank group and the NC group ($P > 0.05$). Compared with the blank and NC groups, the proliferation rate of cells in the miR-141 mimics group and siRNA-Rho group was significantly accelerated ($P < 0.05$), and the rate of cells in the miR-141 inhibitors group was decreased ($P < 0.05$); no significant difference was detected in the miR-141 inhibitors + siRNA-Rho group on proliferation rate ($P > 0.05$) (Fig. 4D).

Comparison of cell cycle and apoptosis in each group after transfection

The PI staining was used to determine the cell cycle. The cell proportion at the G0/G1 phase in the normal group, the blank group, the NC group, the miR-141 mimics group, the miR-141 inhibitors group, the siRNA-Rho group and the miR-141 inhibitors + siRNA-Rho group was 76.23% ± 2.06%, 50.26% ± 3.13% , 51.32% ± 2.36%, 38.26% ± 2.31%, 65.35% ± 2.16%, 41.39% ± 2.42%, and 51.25% ± 2.52%, respectively. The cells proportion at the S phase was 18.36% ± 3.23%, 37.63% ± 2.28%, 35.26% ± 2.39%, 49.36% ± 3.28%, 25.03% ± 3.13%, 48.34% ± 2.76%, and 36.23% ± 2.18%, respectively. Compared with the normal group, the proportion of cells at the G0/G1 phase was decreased and cells at the S phase were increased in other groups (all $P < 0.05$). Compared with the NC and the blank groups, the proportion

of cells at the G0/G1 phase was decreased and cells at the S phase were increased in the miR-141 mimics group and the siRNA-Rho group (both $P < 0.05$); the proportion of cells at the G0/G1 phase was increased and cells at the S phase were decreased in the miR-141 inhibitors group ($P < 0.05$); changes of cell cycles in the miR-141 inhibitors + siRNA-Rho group showed no difference ($P > 0.05$) (Fig. 5).

The Annexin V-FITC/PI double staining was used to measure the apoptosis of cells. The apoptosis rates in the normal group, the blank group, the NC group, the miR-141 mimics group, the miR-141 inhibitors group, the siRNA-Rho group and miR-141 inhibitors + siRNA-Rho group were 5.55% ± 1.95%, 37.64% ± 3.25%, 38.35% ± 2.89%, 27.33% ± 3.26%, 49.12% ± 2.63%, 26.14% ± 1.49%, and 40.82% ± 2.38%, respectively. Compared with the normal group, the apoptosis rate in the other groups was markedly increased (all $P < 0.05$). The apoptosis rate was comparable between the blank group and the NC group ($P > 0.05$). Compared with the NC and the blank groups, the apoptosis rates in the miR-141 mimics group and the siRNA-Rho group were decreased significantly, while were increased in the miR-141 inhibitors group ($P < 0.05$); the apoptosis rate in miR-141 inhibitors + siRNA-Rho group showed insignificant difference ($P > 0.05$) (Fig. 6).

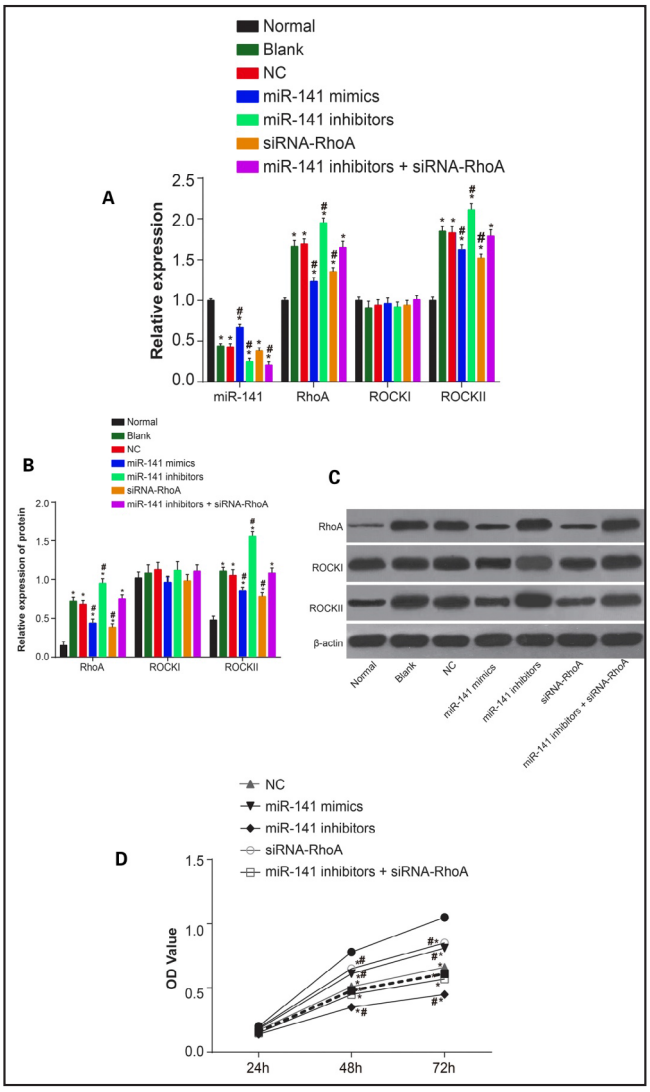

Fig. 4. miR-141 and mRNA of related proteins in the RhoA/ROCK signaling pathway. A: expressions of miR-141 and mRNA of related proteins; B: protein expressions RhoA, ROCK1 and ROCK2 in cells after transfection, statistical analysis chart for protein expressions of RhoA, ROCK1 and ROCK2 of cells; C: Western blotting for protein expressions of RhoA, ROCK1 and ROCK2 of cells; D: changes of cell proliferation after cell transfection. * P<0.05 compared with the normal group; # P<0.05 compared with the blank and the NC groups.

Discussion

Occurrence of DMED largely involves neural, vascular and smooth muscle lesions [16]. Type 1 and type 2 DM are related to the alterations in the level of several miRs in insulin-secreting cells as well as in insulin-target tissues [17]. However, miR141 correlation with DM or DMED is still unknown. Decreased miR141 expression has been correlated to other pathologies such as renal cell carcinoma cancer [18]. miR-141 expression was also obviously decreased in pancreatic cancer tissues [19].

RhoA and ROCK2 have been implicated in plentiful axonal guidance events in the development, such as involvement in the ephrin signaling, the repulsive guidance molecule

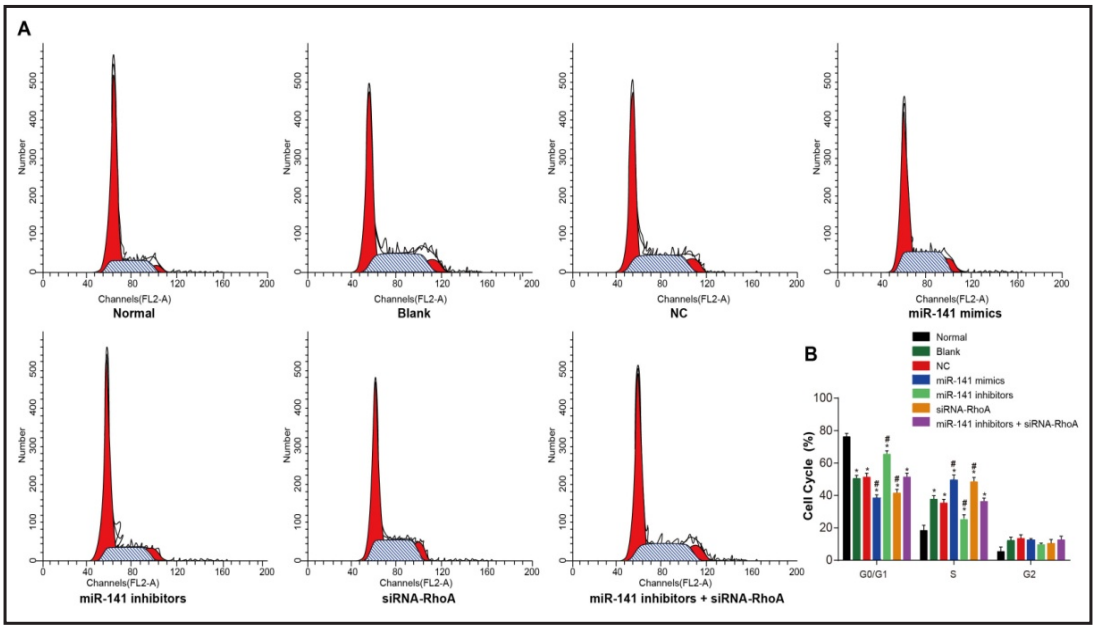

Fig. 5. Cell cycle in each group after cell transfection. The PI staining was used to determine the cell cycle. The cell proportions at the G0/G1 phase and the S phase in the normal group, the blank group, the NC group, the miR-141 mimics group, the miR-141 inhibitors group, the siRNA-Rho group and the miR-141 inhibitors + siRNA-Rho group were presented. Compared with the normal group, the proportion of cells at the G0/G1 phase was decreased and cells at the S phase were increased in other groups (all P<0.05). Compared with the NC and the blank groups, the proportion of cells at the G0/G1 phase was decreased and cells at the S phase were increased in the miR-141 mimics group and the siRNA-Rho group (both P<0.05); the proportion of cells at the G0/G1 phase was increased and cells at the S phase were decreased in the miR-141 inhibitors group (P<0.05); changes of cell cycles in miR-141 inhibitors + siRNA-Rho group showed no difference (P > 0.05). A: cell cycle diagram; B: percentage of cell cycle. * P<0.05 compared with the normal group; # P<0.05 compared with the blank and the NC groups.

(RGM) signaling, and the lysophosphatidic acid (LPA) signaling [20]. Rho associated proteins are involved in an abundant of cell processes, containing proliferation, cytoskeletal actin remodeling, differentiation, and the generation of ROS [21]. ROCK2 is one of isoforms of ROCK and the down-stream effector of RhoA which enhances cell motility via inhibition of myosin phosphatase [20, 22]. One study on the RhoA and RhoGDI at 21 and 27 kDa in the mouse penile tissue showed that the protein expression of ROCKs was significantly increased in the corpus cavernosum tissue from eNOS deficient mice [23]. Hyperglycemia has been reported to up-regulate the RhoA/ROCK pathway in gastric smooth muscle [24].

In our study, we first measured the expressions of miR-141 and the changes of the RhoA/ROCK signaling pathways in the corpus cavernosum tissue of rats with diabetic ED and we found decreased expressions of miR-141 associated with up-regulation of RhoA and ROCK2. RhoA and ROCK2 genes were also highly expressed in rats with DMED. The role of RhoA/ROCK pathway in the regulation of muscle contraction is well established in both visceral and vascular smooth muscle. Most current medical therapies for ED seek to maximize the endogenous signaling of NO. Certain etiologies like diabetes, however, are difficult to treat with current modalities. Thus new molecular targets are in urgent need [25]. Researchers have demonstrated the importance of the RhoA/ROCK signaling pathway in maintaining a flaccid state of the penile, and inhibition of the signaling potentiates smooth muscle relaxation in an NO-independent manner [26].

To further elucidate the link between miR-141 and the RhoA/ROCK signaling pathway, we identified Rho as the direct target genes of miR-141 by bioinformatics methods and then examined the mechanisms that lead to changes in miR-141 and RhoA/ROCK pathway.

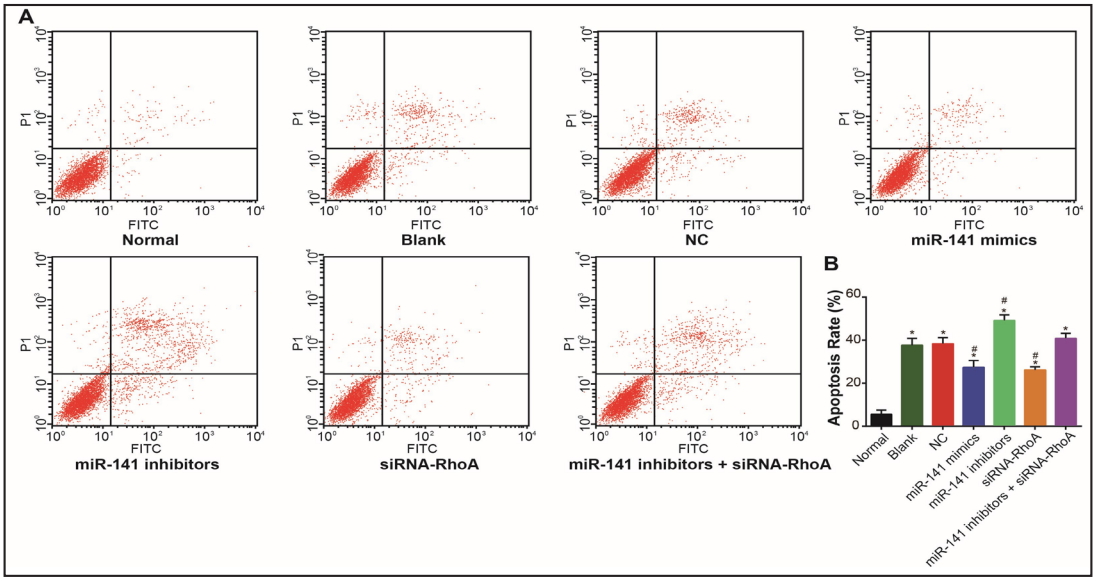

Fig. 6. Cell apoptosis rate after cell transfection. The Annexin V-FITC/PI double staining was used to measure the apoptosis of cells. The apoptosis rates in the normal group, the blank group, the NC group, the miR-141 mimics group, the miR-141 inhibitors group, the siRNA-Rho group and miR-141 inhibitors + siRNA-Rho group were presented. Compared with the normal group, the apoptosis rate in other groups was markedly increased (all $P<0.05$). The apoptosis rate was comparable between the blank group and NC group ($P > 0.05$). Compared with the NC and the blank groups, the apoptosis rates in the miR-141 mimics group and the siRNA-Rho group were decreased significantly, while were increased in the miR-141 inhibitors group ($P<0.05$); the apoptosis rate in miR-141 inhibitors + siRNA-Rho group showed insignificant difference ($P > 0.05$). A: cell apoptosis diagram; B: percentage of apoptotic cells. * $P<0.05$ compared with the normal group; # $P<0.05$ compared with the blank and the NC groups.

We investigated the effects of miR-141 on the RhoA/ROCK signaling pathway *in vitro*. Up-regulated expression of miR-141 inhibited the growth of penile cavernous smooth muscle cells associated with down-regulation of the RhoA/ROCK pathway *in vitro*. The expressions of RhoA and ROCK2 were increased in the cells transfected with miR-141 inhibitors. Previously, we reported that AngII silencing may improve erectile function of diabetic rats via down-regulating the RhoA/ROCK signaling pathway [27]. miR-141 may target RhoA whereby playing a role in transcriptional regulation. ROCK2 appears to be a down-stream effector of RhoA and the RhoA/ROCK signaling pathway might serve as a promising target for the treatment of DMED. miR-141 may inhibit the RhoA/ROCK signaling pathway by reducing the expression of ROCK. Taken together, our studies provide a link between miR-141, ROCK and DMED.

We showed increased RhoA protein by immunostaining only, and RhoA and ROCK by Western blotting only. However, increased expression not necessarily indicates increased activity. In our parallel study, we found that ripasudil, a selective ROCK inhibitor, could improve the erectile function in diabetic rats (unpublished data). Our findings, alongside with those from a previous report [28], indicate that DMED can be alleviated by suppressing the activity of ROCK2.

In summary, decreased expression of miR-141 was associated with up-regulation of RhoA and ROCK2 in the RhoA/ROCK signaling pathway in DMED. miR-141 inhibits the growth of penile cavernous smooth muscle cells associated with down-regulation of the RhoA/Rho kinase signaling pathway *in vitro*. The RhoA/ROCK signaling pathway might be a promising target for the treatment of DMED.

Acknowledgements

The study was supported by funding from Jilin University.

Disclosure Statement

No conflicts of interest exist.

References

1 Shaw JE, Sicree RA, Zimmet PZ: Global estimates of the prevalence of diabetes for 2010 and 2030. Diabetes Res Clin Pract 2010;87:4-14.
2 Stefek M: Natural flavonoids as potential multifunctional agents in prevention of diabetic cataract. Interdiscip Toxicol 2011;4:69-77.
3 Braun M, Wassmer G, Klotz T, Reifenrath B, Mathers M, Engelmann U: Epidemiology of erectile dysfunction: results of the 'Cologne Male Survey'. Int J Impot Res 2000;12:305-311.
4 Al-Kuraishy HM, Al-Gareeb AI: Erectile Dysfunction and Low Sex Drive in Men with Type 2 DM: The Potential Role of Diabetic Pharmacotherapy. J Clin Diagn Res 2016;10:FC21-FC26.
5 Minami H, Furukawa S, Sakai T, Niiya T, Miyaoka H, Miyake T, Yamamoto S, Kanzaki S, Maruyama K, Tanaka K, Ueda T, Senba H, Torisu M, Tanigawa T, Matsuura B, Hiasa Y, Miyake Y: Physical activity and prevalence of erectile dysfunction in Japanese patients with type 2 diabetes mellitus: The Dogo Study. J Diabetes Investig 2018;9:193-198
6 Ogbera OA, Sonny C, Olufemi F, Wale A: Hypogonadism and subnormal total testosterone levels in men with type 2 diabetes mellitus. J Coll Physicians Surg Pak 2011;21:517-521.
7 Pop-Busui R, Hotaling J, Braffett BH, Cleary PA, Dunn RL, Martin CL, Jacobson AM, Wessells H, Sarma AV; **DCCT/EDIC** Research Group: Cardiovascular autonomic neuropathy, erectile dysfunction and lower urinary tract symptoms in men with type 1 diabetes: findings from the DCCT/EDIC. J Urol 2015;193:2045-2051.
8 Okumura N, Fujii K, Kagami T, Makiko N, Kitahara M, Kinoshita S, Koizumi N: Activation of the RhoA/Rho Kinase Signaling Pathway Is Involved in Cell Death of Corneal Endothelium. Invest Ophthalmol Vis Sci 2016;57:6843-6851.
9 Uvin P, Albersen M, Bollen I, Falter M, Weyne E, Linsen L, Tinel H, Sandner P, Bivalacqua TJ, De Ridder DJ, Van der Aa F, Brône B, Van Renterghem K: Additive effects of the Rho kinase inhibitor Y-27632 and vardenafil on relaxation of the corpus cavernosum tissue of patients with erectile dysfunction and clinical phosphodiesterase type 5 inhibitor failure. BJU Int 2017;119(2):325-332.
10 Luppi F, Beghe B, Richeldi L: Acute exacerbations of chronic obstructive pulmonary disease: are antibiotics needed? Am J Respir Crit Care Med 2010;181:102-103.
11 Sun Y, Lu CM, Song Z, Xu KK, Wu SB, Li ZJ: Expression and regulation of microRNA-29a and microRNA-29c in early diabetic rat cataract formation. Int J Ophthalmol 2016;9:1719-1724.
12 Li DS, Feng L, Luo LH, Duan ZF, Li XL, Yin CH, Sun X: The Effect of microRNA-328 antagomir on erectile dysfunction in streptozotocin-induced diabetic rats. Biomed Pharmacother 2017;92:888-895.
13 Zhang L, Deng T, Li X, Liu H, Zhou H, Ma J, Wu M, Zhou M, Shen S, Li X, Niu Z, Zhang W, Shi L, Xiang B, Lu J, Wang L, Li D, Tang H, Li G: microRNA-141 is involved in a nasopharyngeal carcinoma-related genes network. Carcinogenesis 2010;31:559-566.
14 Saito S, Thuc LC, Teshima Y, Nakada C, Nishio S, Kondo H, Fukui A, Abe I, Ebata Y, Saikawa T, Moriyama M, Takahashi N: Glucose Fluctuations Aggravate Cardiac Susceptibility to Ischemia/Reperfusion Injury by Modulating MicroRNAs Expression. Circ J 2016;80:186-195.
15 Pan F, Xu J, Zhang Q, Qiu X, Yu W, Xia J, Chen T, Pan L, Chen Y, Dai Y: Identification and characterization of the MicroRNA profile in aging rats with erectile dysfunction. J Sex Med 2014;11:1646-1656.
16 He Y, He W, Qin G, Luo J, Xiao M: Transplantation KCNMA1 modified bone marrow-mesenchymal stem cell therapy for diabetes mellitus-induced erectile dysfunction. Andrologia 2014;46:479-486.

17 Guay C, Roggli E, Nesca V, Jacovetti C, Regazzi R: Diabetes mellitus, a microRNA-related disease? Transl Res 2011;157:253-264.
18 Chen X, Wang X, Ruan A, Han W, Zhao Y, Lu X, Xiao P, Shi H, Wang R, Chen L, Chen S, Du Q, Yang H, Zhang X: miR-141 is a key regulator of renal cell carcinoma proliferation and metastasis by controlling EphA2 expression. Clin Cancer Res 2014;20:2617-2630.
19 Zhao G, Wang B, Liu Y, Zhang JG, Deng SC, Qin Q, Tian K, Li X, Zhu S, Niu Y, Gong Q, Wang CY: miRNA-141, downregulated in pancreatic cancer, inhibits cell proliferation and invasion by directly targeting MAP4K4. Mol Cancer Ther 2013;12:2569-2580.
20 Duffy P, Schmandke A, Schmandke A, Sigworth J, Narumiya S, Cafferty WB, Strittmatter SM: Rho-associated kinase II (ROCKII) limits axonal growth after trauma within the adult mouse spinal cord. J Neurosci 2009;29:15266-15276.
21 Wu XD, Liu WL, Zeng K, Lei HY, Zhang QG, Zhou SQ, Xu SY: Advanced glycation end products activate the miRNA/RhoA/ROCK2 pathway in endothelial cells. Microcirculation 2014;21:178-186.
22 Hong J, Li D, Cao W: Rho Kinase ROCK2 Mediates Acid-Induced NADPH Oxidase NOX5-S Expression in Human Esophageal Adenocarcinoma Cells. PLoS One 2016;11:e0149735.
23 Priviero FB, Jin LM, Ying Z, Teixeira CE, Webb RC: Up-regulation of the RhoA/Rho-kinase signaling pathway in corpus cavernosum from endothelial nitric-oxide synthase (NOS), but not neuronal NOS, null mice. J Pharmacol Exp Ther 2010;333:184-192.
24 Mahavadi S, Sriwai W, Manion O, Grider JR, Murthy KS: Diabetes-induced oxidative stress mediates upregulation of RhoA/Rho kinase pathway and hypercontractility of gastric smooth muscle. PLoS One 2017;12:e0178574.
25 Sopko NA, Hannan JL, Bivalacqua TJ:
Understanding and targeting the Rho kinase pathway in erectile dysfunction. Nat Rev Urol 2014;11:622-628.
26 Thoma C: Erectile dysfunction: Too much ROCK - erection block. Nat Rev Urol 2017;14:6.
27 Zhang Y, Jia L, Zhang Y, Ji W, Li H: Angiotensin II Silencing Alleviates Erectile Dysfunction Through Down-Regulating the Rhoa/Rho Kinase Signaling Pathway in Rats with Diabetes Mellitus. Cell Physiol Biochem 2018;45:419-427.
28 Sezen SF, Lagoda G, Musicki B, Burnett AL: Hydroxyl fasudil, an inhibitor of Rho signaling,
improves erectile function in diabetic rats: a role for neuronal ROCK. J Sex Med 2014;11:2164-2171.